XII. STATISTICAL COMMUNICATION THEORY*

Prof. Y. W. Lee
Prof. A. G. Bose
Prof. D. J. Sakrison
Prof. M. Schetzen
Prof. H. L. Van Trees
V. R. Algazi
R. Alter
D. S. Arnstein
M. E. Austin
R. F. Bauer
E. M. Bregstone
J. D. Bruce
A. M. Bush
J. K. Clemens
A. G. Gann
L. M. Goodman
C. E. Gray
T. G. Kincaid
A. J. Kramer
D. E. Nelsen
J. K. Omura
A. V. Oppenheim
R. B. Parente
J. S. Richters
W. S. Smith, Jr.
D. W. Steele

A. WORK COMPLETED

1. A STUDY OF THE PERFORMANCE OF LINEAR AND NONLINEAR SYSTEMS

This study has been completed by V. R. Algazi. In August 1963 he submitted the results to the Department of Electrical Engineering, M. I. T., as a thesis in partial fulfillment of the requirements for the degree of Doctor of Philosophy.

Y. W. Lee

2. DESIGN AND ANALYSIS OF A DC TAPE RECORDING SYSTEM USING TWO-STATE MODULATION

This study has been completed by D. E. Nelsen. In August 1963 he submitted the results to the Department of Electrical Engineering, M. I. T., as a thesis in partial fulfillment of the requirements for the degree of Master of Science.

A. G. Bose

3. ANALOG MULTIPLIER BASED ON A TWO-STATE MODULATION SYSTEM

This study has been completed by C. E. Gray. In August 1963 he submitted the results to the Department of Electrical Engineering, M. I. T., as a thesis in partial fulfillment of the requirements for the degree of Master of Science.

A. G. Bose

4. SYNCHRONOUS RECEIVER FOR DIGITAL MULTI-PHASE MODULATION

This study has been completed by L. M. Goodman. In August 1963 he submitted the results to the Department of Electrical Engineering, M. I. T., as a thesis in partial fulfillment of the requirements for the degree of Master of Science.

H. L. Van Trees

---

*This work was supported in part by the National Institutes of Health (Grant MH-04737-03); and in part by the National Science Foundation (Grant G-16526); additional support was received under NASA Grant NsG-496.

5. A MULTIPLEX COMMUNICATION SYSTEM USING PSEUDO-NOISE CARRIERS

This study has been completed jointly by A. J. Kramer and J. K. Omura. In August 1963 they submitted the results to the Department of Electrical Engineering, M. I. T., as a thesis in partial fulfillment of the requirements for the degree of Master of Science.

H. L. Van Trees

B. MEASUREMENT OF THE KERNELS OF A NONLINEAR SYSTEM OF FINITE ORDER

If a nonlinear system can be characterized by the first p kernels, then the system can be represented in the form of a Volterra series of the p^{th} order

$$y(t) = N_p[x(t)] = \sum_{n=1}^{p} \mathcal{K}_n[x(t)], \tag{1}$$

in which y(t) is the response of the nonlinear system for the input x(t) and

$$\mathcal{K}_n[x(t)] = \int_{-\infty}^{\infty} \cdots \int_{-\infty}^{\infty} h_n(\tau_1, \ldots, \tau_n)\, x(t-\tau_1) \cdots x(t-\tau_n)\, d\tau_1 \cdots d\tau_n. \tag{2}$$

In this report, we shall present an exact method by which the Volterra representation of a nonlinear system that contains only a finite number of kernels can be determined directly.

A first-order system is one in which the highest order kernel is $h_1(\tau_1)$. Such a system is linear and the first-order kernel is the impulse response of the linear system. The technique that we shall present is one whereby each of the Volterra kernels of a p^{th}-order system can be determined individually as a multidimensional impulse response. To explain this technique, we first shall discuss the procedure for determining the Volterra kernels of second- and third-order systems. The generalization of the procedure for p^{th}-order systems will then be given.

1. Second-Order Systems

The Volterra representation of a second-order system is

$$y(t) = N_2[x(t)] = \mathcal{K}_1[x(t)] + \mathcal{K}_2[x(t)]. \tag{3}$$

A schematic representation of such a system is shown in Fig. XII-1. From such a system, we can form a system with the output

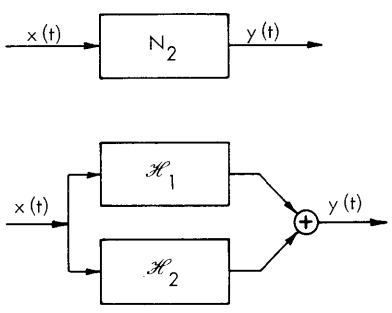

Fig. XII-1. Schematic representations of a second-order system.

$$y_1(t) = \mathcal{K}_1[x(t)], \tag{4}$$

since, from Eq. 2,

$$\mathcal{K}_1[-x(t)] = -\mathcal{K}_1[x(t)]$$

and (5)

$$\mathcal{K}_2[-x(t)] = \mathcal{K}_2[x(t)].$$

Thus the system formed as shown in Fig. XII-2a has the representation given by Eq. 4. Also, the system of Fig. XII-2b has the output

$$y_2(t) = \mathcal{K}_2[x(t)]. \tag{6}$$

A method for measuring such an isolated second-order kernel has been given by George.[1] The method is based upon the observation that

$$g_2(t) = 2\mathcal{K}_2(x_1x_2) = \mathcal{K}_2[x_1+x_2] - \mathcal{K}_2[x_1] - \mathcal{K}_2[x_2], \tag{7}$$

in which, for convenience, we have dropped the argument t and we have defined

$$\mathcal{K}_2(x_1x_2) = \int_{-\infty}^{\infty}\int_{-\infty}^{\infty} h_2(\tau_1,\tau_2)\, x_1(t-\tau_1)\, x_2(t-\tau_2)\, d\tau_1 d\tau_2. \tag{8}$$

Equation 7 can be verified from Eq. 2 by direct substitution. When this is carried out, Eq. 7 follows as a result of the identity

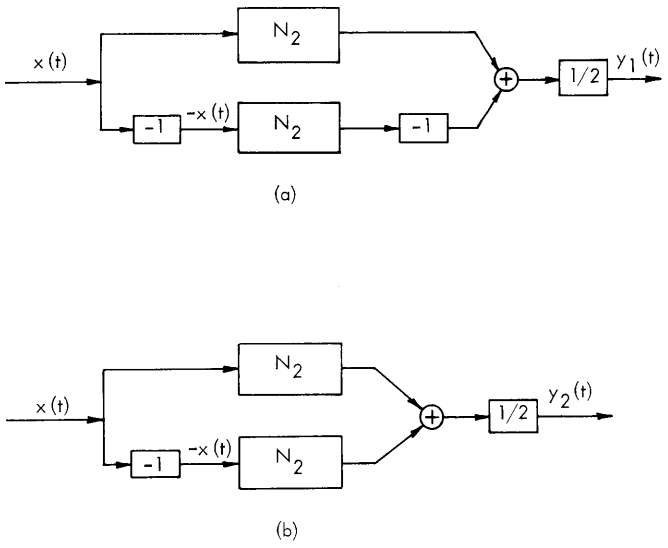

Fig. XII-2. (a) Connections for a second-order system for the output $y_1(t)$.
(b) Connections for a second-order system for the output $y_2(t)$.

$$2x_1x_2 = (x_1+x_2)^2 - \left[x_1^2+x_2^2\right]. \tag{9}$$

A system with the output $g_2(t)$ is shown in Fig. XII-3. Thus if $x_1(t) = u_o(t-T_1)$ and $x_2(t) = u_o(t-T_2)$, then

$$g_2(t) = 2h_2(t-T_1,t-T_2). \tag{10}$$

As shown in Fig. XII-4, this is the second-order impulse response of the kernel $h_2(\tau_1,\tau_2)$ along a 45° line in the τ_1-τ_2 plane.

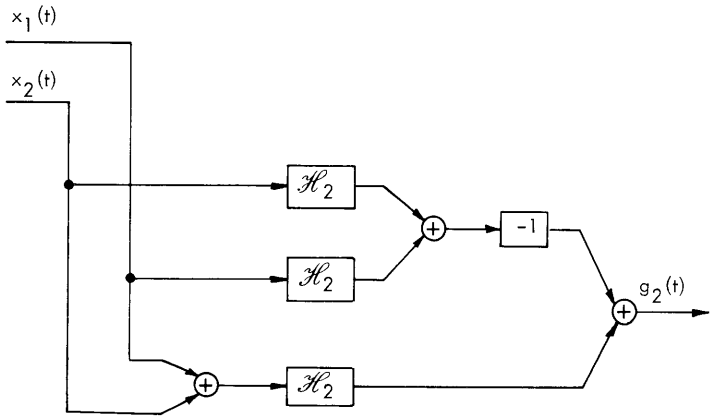

Fig. XII-3. Connections for the system $\mathcal{H}_2$ for the output $g_2(t)$.

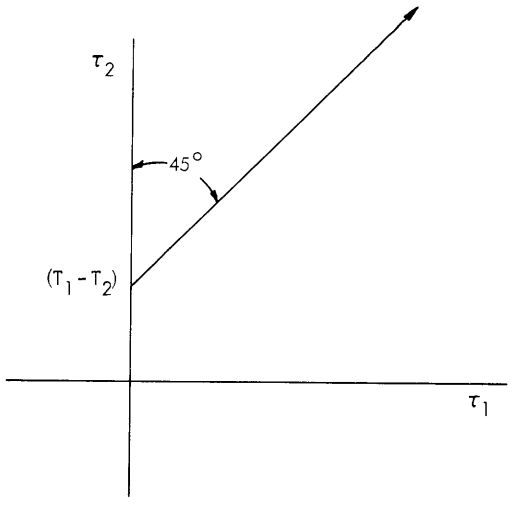

Fig. XII-4. Line of a double-impulse response in the τ_1-τ_2 plane as given by Eq. 10. (Arrow points in the direction of increasing t.)

We now note that we need not have suppressed the first-order kernel, since, from Eqs. 3 and 7,

$$N_2[x_1+x_2] - N_2[x_1] - N_2[x_2] = \mathcal{K}_2[x_1+x_2] - \mathcal{K}_2[x_1] - \mathcal{K}_2[x_2] + \mathcal{K}_1[x_1+x_2] - \mathcal{K}_1[x_1] - \mathcal{K}_1[x_2]$$

$$= g_2(t) \tag{11}$$

and we have made use of the result that

$$\mathcal{K}_1[x_1+x_2] - \mathcal{K}_1[x_1] - \mathcal{K}_1[x_2] = 0. \tag{12}$$

Thus the system formed as shown in Fig. XII-5 also has the output $g_2(t)$. The first-order kernel can be obtained as the impulse response of the system of Fig. XII-2a.

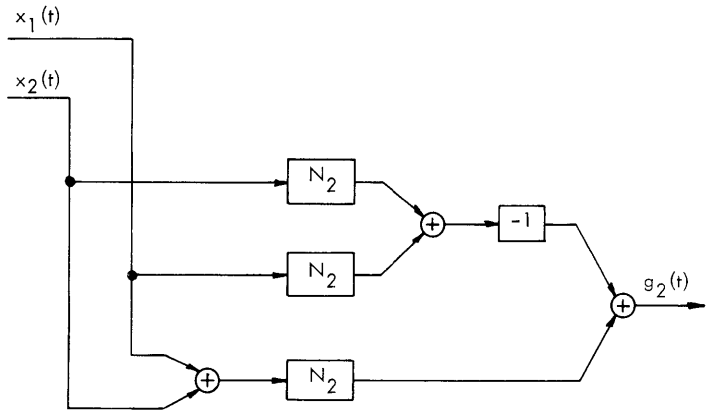

Fig. XII-5. Connections for a general second-order system for the output $g_2(t)$.

Alternatively, from Eq. 3, the impulse response of the second-order system, N_2, is

$$N_2[u_o(t)] = h_1(t) + h_2(t,t). \tag{13}$$

Thus $h_1(\tau_1)$ can be determined from the impulse response of the second-order system once $h_2(\tau_1,\tau_2)$ is known.

2. Third-Order Systems

The Volterra representation of a third-order system is

$$y(t) = N_3[x(t)] = \mathcal{K}_1[x(t)] + \mathcal{K}_2[x(t)] + \mathcal{K}_3[x(t)]. \tag{14}$$

Let us begin by considering the special case of a third-order system containing an isolated third-order kernel, that is, we first shall consider the case for which

$$y(t) = N_3[x(t)] = \mathcal{K}_3[x(t)]. \tag{15}$$

A method for measuring such an isolated third-order kernel is obtained from the identity

$$g_3(t) = 3!\, \mathcal{K}_3(x_1x_2x_3)$$

$$= \mathcal{K}_3[x_1+x_2+x_3] - \mathcal{K}_3[x_1+x_2] - \mathcal{K}_3[x_2+x_3]$$

$$- \mathcal{K}_3[x_3+x_1] + \mathcal{K}_3[x_1] + \mathcal{K}_3[x_2] + \mathcal{K}_3[x_3], \tag{16}$$

in which we have defined

$$\mathcal{K}_3(x_1x_2x_3) = \int_{-\infty}^{\infty}\int_{-\infty}^{\infty}\int_{-\infty}^{\infty} h_3(\tau_1,\tau_2,\tau_3)\, x_1(t-\tau_1)\, x_2(t-\tau_2)\, x_3(t-\tau_3)\, d\tau_1 d\tau_2 d\tau_3. \tag{17}$$

Equation 16 can be verified by direct substitution in Eq. 2. When this is carried out Eq. 16 follows as a result of the identity

$$3!\, x_1x_2x_3 = (x_1+x_2+x_3)^3 - \left[(x_1+x_2)^3+(x_2+x_3)^3+(x_3+x_1)^3\right] + \left[x_1^3+x_2^3+x_3^3\right]. \tag{18}$$

A system with the output $g_3(t)$ is shown in Fig. XII-6. Thus if $x_1(t) = u_o(t-T_1)$, $x_2(t) = u_o(t-T_2)$, and $x_3(t) = u_o(t-T_3)$, then

$$g_3(t) = 3!\, h_3(t-T_1, t-T_2, t-T_3). \tag{19}$$

This is the third-order impulse response of the kernel $h_3(\tau_1,\tau_2,\tau_3)$ along a line that is at 45° with each of the coordinate axes in the τ_1-τ_2-τ_3 space. Any such 45° line in the τ_1-τ_2-τ_3 space can be obtained by a proper choice of delays T_1, T_2, and T_3.

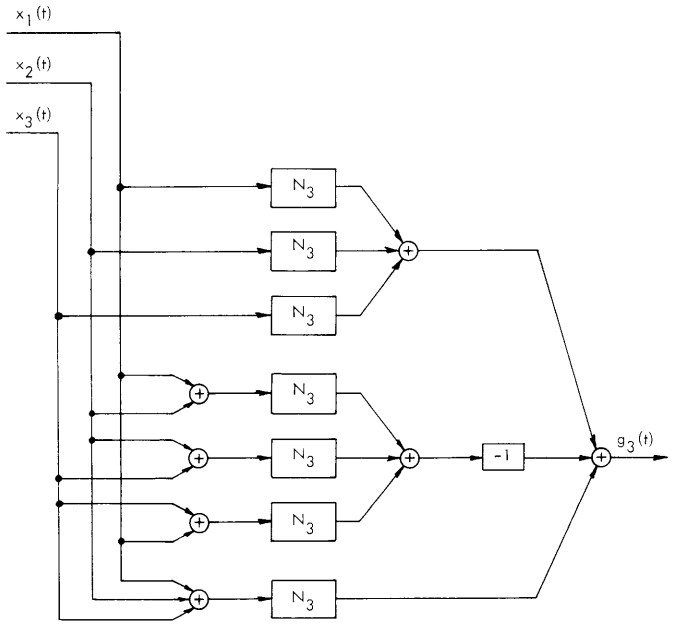

Fig. XII-6. Connections for a third-order system for the output $g_3(t)$.

Now, if the third-order system of Fig. XII-6 also contains a first- and a second-order kernel, then the output still will be $g_3(t)$, as given by Eq. 16. To observe this, we note that the output resulting from the presence of a first-order kernel is zero, since

$$\mathcal{K}_1[x_1+x_2+x_3] - \mathcal{K}_1[x_1+x_2] - \mathcal{K}_1[x_2+x_3] - \mathcal{K}_1[x_3+x_1] + \mathcal{K}_1[x_1] + \mathcal{K}_1[x_2] + \mathcal{K}_1[x_3] = 0. \tag{20}$$

Equation 20 follows as a result of the identity

$$(x_1+x_2+x_3) - [(x_1+x_2)+(x_2+x_3)+(x_3+x_1)] + [x_1+x_2+x_3] = 0. \tag{21}$$

Also, the output resulting from the presence of a second-order kernel is zero, since

$$\mathcal{K}_2[x_1+x_2+x_3] - \mathcal{K}_2[x_1+x_2] - \mathcal{K}_2[x_2+x_3] - \mathcal{K}_2[x_3+x_1] + \mathcal{K}_2[x_1] + \mathcal{K}_2[x_2] + \mathcal{K}_2[x_3] = 0. \tag{22}$$

Equation 22 follows as a result of the identity

$$(x_1+x_2+x_3)^2 - \left[(x_1+x_2)^2+(x_2+x_3)^2+(x_3+x_1)^2\right] + \left[x_1^2+x_2^2+x_3^2\right] = 0. \tag{23}$$

Thus the system shown in Fig. XII-6 has the output $g_3(t)$ as given by Eq. 16, even in the case in which N_3 is a general third-order system. The third-order Volterra kernel can thus be obtained by means of the circuit of Fig. XII-6, as the third-order impulse response given by Eq. 19. One method of obtaining the first- and second-order kernels is to subtract the third-order kernel from the third-order system, N_3. The result is a second-order system, N_2, whose kernels can be determined by the methods described in the previous section.

3. p^{th}-Order Systems

The Volterra representation of a p^{th}-order system, N_p, is given by Eq. 1. From our previous discussion of second- and third-order systems, the approach is to form, from the system N_p, a system whose output is $H_p(x_1, \ldots, x_p)$. This was accomplished for third-order systems as a result of the polynomial identities (18), (21), and (23). In fact, the form of the system of Fig. XII-6 is immediately apparent from identity (18). The fact that the output of the system of Fig. XII-6 which is due to the second- and third-order kernels is zero is a consequence of identities (21) and (23). The result for p^{th}-order systems follows from a generalization of these polynomial identities. However, before discussing the general polynomial identity, we shall discuss the identity that we consider for a fourth-order system. The identity for $P = 4$ is

$$4!\, x_1x_2x_3x_4 = (x_1+\ldots+x_4)^4 - \left[(x_1+x_2+x_3)^4+\ldots\right] + \left[(x_1+x_2)^4+\ldots\right] - \left[x_1^4+\ldots+x_4^4\right]. \tag{24}$$

Each term in the second term of Eq. 24 is the sum of three different x's raised to the fourth power. The second term, then, is the sum of all distinctly different such terms. There are $\binom{4}{3} = 4$ such terms. Each term in the third term of Eq. 24 is the sum of two different x's raised to the fourth power. The third term, then, is the sum of all distinctly different such terms. There are $\binom{4}{2} = 6$ such terms. Finally, each term in the fourth term of Eq. 24 is an individual x raised to the fourth power. The fourth term, then, is the sum of all distinctly different such terms. There are $\binom{4}{1} = 4$ such terms. The total number of terms in Eq. 24 is thus $\binom{4}{1} + \binom{4}{2} + \binom{4}{3} + \binom{4}{4} = 2^4 - 1 = 15$.

We now can show that if we form, from a fourth-order system, a system according to Eq. 24, the output will be $4!\ \mathcal{K}_4(x_1x_2x_3x_4)$. This is because the output resulting from the first-, second-, and third-order kernels will be zero. To show this, we need to show that the right-hand side of Eq. 24 is zero if each term is raised to a power that is less than four. That is, we must show that

$$(x_1+\ldots+x_4)^n - \left[(x_1+x_2+x_3)^n+\ldots\right] + \left[(x_1+x_2)^n+\ldots\right] - \left[x_1^n+\ldots+x_4^n\right] = 0 \qquad \text{for } n = 1,2,3. \tag{25}$$

This identity is seen by differentiating Eq. 24 with respect to x_1. The result is

$$3!\ x_2x_3x_4 = (x_1+\ldots+x_4)^3 - \left[(x_1+x_2+x_3)^3+\ldots\right] + \left[(x_1+x_2)^3+\ldots\right] - x_1^3. \tag{26}$$

Compare Eq. 25 for n = 3 with Eq. 26. The right-hand side of Eq. 26 is identical with Eq. 25 except that terms that do not contain x_1 are missing. Thus as a function of x_1, both equations are identical. However, the left-hand side of Eq. 26 is not a function of x_1. Thus as a function of x_1, Eq. 25 for n = 3 is a constant. Similarly, Eq. 25 for n = 3 is a constant as a function of x_2, x_3, and x_4. Equation 25 is thus, at most, a constant. The constant, however, is seen to be zero by considering the case for which $x_1 = x_2 = x_3 = x_4 = 0$. Thus Eq. 25 is valid for n = 3. To show that Eq. 25 is also valid for n = 2, we differentiate Eq. 26 with respect to x_1. We then obtain

$$0 = (x_1+\ldots+x_4)^2 - \left[(x_1+x_2+x_3)^2+\ldots\right] + \left[(x_1+x_2)^2+\ldots\right] - x_1^2. \tag{27}$$

By an argument similar to that for n = 3, we establish the validity of Eq. 25 for n = 2. Similarly, we can show that Eq. 25 is also valid for n = 1 by differentiating Eq. 27 with respect to x_1. Thus, if we form, from a fourth-order system, a system according to Eq. 24, the output resulting from the first-, second- and third-order kernels will be zero and the output that is due to the fourth-order kernel will be

$$g_4(t) = 4!\ \mathcal{K}_4(x_1x_2x_3x_4). \tag{28}$$

By choosing each x to be a unit impulse, the fourth-order kernel can be obtained as a

fourth-order impulse response. One method of obtaining the kernels of order less than four is to subtract the fourth-order kernel from the fourth-order system. The result is a third-order system, whose kernels can be determined by the methods described previously.

Now consider the general case for a p^{th}-order system. To obtain a system whose output is

$$g_p(t) = p!\, \mathcal{K}_p(x_1 \ldots x_p), \tag{29}$$

we form, from the p^{th}-order system, a system according to the identity

$$p!\, x_1 \ldots x_p = (x_1 + \ldots + x_p)^p - [(x_1 + \ldots + x_{p-1})^p + \ldots] + [(x_1 + \ldots + x_{p-2})^p + \ldots]$$

$$+ \ldots + (-1)^{p-1}\left[x_1^p + \ldots + x_p^p\right]. \tag{30}$$

Each term in the second term of Eq. 30 is the sum of (p-1) different x's raised to the p^{th} power; thus the second term is the sum of all distinctly different such terms. There are $\binom{p}{p-1} = p$ such terms. Each term in the third term of Eq. 30 is the sum of (p-2) different x's raised to the p^{th} power; thus the third term is the sum of all distinctly different such terms. There are $\binom{p}{p-2} = \frac{(p)(p-1)}{2}$ such terms. Similarly, for all of the terms of Eq. 30, the last term is the p^{th} term in which each term is an individual x raised to the p^{th} power; thus the p^{th} term is the sum of all distinctly different such terms. There are $\binom{p}{1} = p$ such terms. The total number of terms, M_p, in Eq. 30 thus is

$$M_p = \sum_{n=1}^{p} \binom{p}{n} = 2^p - 1. \tag{31}$$

The output of such a system will be as given by Eq. 29, since the output that is due to the kernels of order less than p is zero. This follows from the result that

$$(x_1 + \ldots + x_p)^n - [(x_1 + \ldots + x_{p-1})^n + \ldots] + \ldots + (-1)^{p-1}\left[x_1^n + \ldots + x_p^n\right] = 0$$

$$\text{for } n = 1, \ldots, p-1. \tag{32}$$

The validity of Eq. 32 can be established by differentiation of Eq. 30 in exactly the same manner as for p = 4.

Thus, if we form, from a p^{th}-order system, a system according to Eq. 30, the output that is due to the first- through the $(p-1)^{th}$-order kernels will be zero, and the output that is due to the p^{th}-order kernel will be given by Eq. 29. By choosing each input, $x_n(t)$, to be a unit impulse, the p^{th}-order kernel can be obtained as a p^{th}-order impulse response. Also, the p-dimensional kernel transform can be obtained experimentally by choosing each input, $x_n(t)$, to be a sinusoid. One method of obtaining the kernels of

order less than p is to subtract the p^{th}-order kernel from the p^{th}-order system. The result is a $(p-1)^{th}$-order system. In this manner, each kernel can be determined successively from the highest-order to the first-order kernel.

4. Suppression of Kernels

We have indicated that each kernel can be determined successively. However, if all of the kernels of a p^{th}-order system are to be determined, the measurements of the lower-order kernels can be simplified by initially suppressing all of the even- or odd-order kernels. This can be accomplished, since from Eq. 2

$$\mathcal{K}_{2n}[x(t)] = \mathcal{K}_{2n}[-x(t)] \tag{33a}$$

and

$$\mathcal{K}_{2n+1}[x(t)] = -\mathcal{K}_{2n+1}[-x(t)]. \tag{33b}$$

Thus the system formed as shown in Fig. XII-7b contains no even-order kernels. Also, the system formed as shown in Fig. XII-7a contains no odd-order kernels. Thus, for example, to measure the second-order kernel of a third-order system, we need not subtract the third-order kernel from the system to form a second-order system. Rather, the third- and first-order kernels can be suppressed by forming a system as depicted in Fig. XII-7a. The second-order kernel then can be measured by forming, from the resulting system, a system as shown in Fig. XII-5.

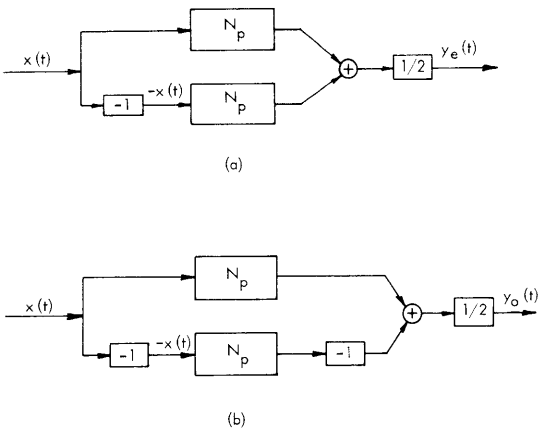

Fig. XII-7. (a) Connections for a p^{th}-order system to suppress the response resulting from odd-order kernels.
(b) Connections for a p^{th}-order system to suppress the response resulting from even-order kernels.

The techniques described in this report are also useful in the synthesis of desired nonlinear systems. For example, in the design of square-law devices, it is sufficient for many purposes to suppress odd-order kernels by means of the system of Fig. XII-7a. However, any set of kernels of a p^{th}-order system can be suppressed by the use of the systems that we have described.

5. Some Measurement Techniques

Our discussion thus far would seem to indicate that, to measure a p^{th}-order kernel, we would require 2^p-1 identical p^{th}-order systems. However, we could, instead, perform 2^p-1 measurements on one such system and then add the outputs in the manner indicated by Eq. 30. If this procedure is carried out, then some of the

measurement will be redundant. For example, if each input, $x_n(t)$, is an impulse, then the response of the p^{th}-order system for $x_1(t)$ is the same as for $x_2(t)$ except for a shift in time. Thus to obtain $g_p(t)$ as given by Eq. 29, only one measurement is needed to determine the function that corresponds to the last term of Eq. 30. Thus, at most, 2^p-p separate measurements are required. For certain relations among the delays, T_n, other redundancies will arise. The minimum number of required measurements is p, which corresponds to the case in which all delays are equal so that $g_p(t) = p!\, h_p(t, t, \ldots, t)$.

The analysis that we have presented is exact for p^{th}-order systems. However, the representation of a nonlinear system as a p^{th}-order system may be adequate for only a limited range of input amplitudes. There are cases in which this range is sufficiently small so that the analysis of the nonlinear system by means of very narrow pulses, which approximate impulses, is not practical. An example is certain electronic systems that can be considered linear only for inputs of small amplitudes. One technique that is used in such cases is to obtain the step response of the system; the derivative of the step response is the desired impulse response. We shall now present an extension of this technique to systems that can be considered to be of the p^{th} order for a limited range of input amplitudes. If we form, from such a system, a system according to Eq. 30, then the output that is due to the first- through the $(p-1)^{th}$-order kernels will be zero, and the output that is due to the p^{th}-order kernel will be given by Eq. 29. Furthermore, if each of the inputs is within a limited range, then the output that is due to the kernels of order greater than p can be neglected. An input that can be used in such cases is the step. Let

$$x_n(t) = a u_{-1}(t-T_n), \tag{34}$$

in which $u_{-1}(t-T_n)$ is a unit step that starts at $t = T_n$. The output for such an input is

$$s_p(t) = a^p p! \int_{-\infty}^{t-T_1} \cdots \int_{-\infty}^{t-T_p} h_p(\tau_1, \ldots, \tau_p)\, d\tau_1, \ldots, d\tau_p. \tag{35}$$

Consider the difference

$$s_p(t+\delta) - s_p(t) = a^p p! \int_{t-T_1}^{t-T_1+\delta} \cdots \int_{t-T_p}^{t-T_p+\delta} h_p(\tau_1, \ldots, \tau_p)\, d\tau_1, \ldots, d\tau_p. \tag{36}$$

Let δ be small so that we can consider $h_p(\tau_1, \ldots, \tau_p)$ essentially constant in the range $t - T_n \leq \tau_n \leq t - T_n + \delta$. Then

$$\frac{s_p(t+\delta) - s_p(t)}{a^p \delta^p} \approx p!\, h_p(t-T_1, \ldots, t-T_p) = g_p(t). \tag{37}$$

For p = 1, Eq. 37 reduces to

$$g_1(t) = \frac{1}{a} s_1'(t), \tag{38}$$

which is the usual result for linear systems. Thus if the input to the nonlinear system is restricted in amplitude, the p-dimensional impulse response, $g_p(t)$, can be obtained from the p-dimensional step response, $s_p(t)$, by means of Eq. 37.

M. Schetzen

References

1. D. A. George, Continuous Nonlinear Systems, Technical Report 355, Research Laboratory of Electronics, M.I.T., July 24, 1959, pp. 6-7.

C. A METHOD OF CONSTRUCTING FUNCTION GENERATORS

In this report we shall describe a method for the construction of function generators. The method is based upon the fact that the average value of a periodic train of pulses is the area of one pulse divided by the period. Consider the negative triangular wave, $g_a(t)$, of amplitude E and period T shown in Fig. XII-8a. By adding a dc voltage, v, to the triangular wave and half-wave rectifying the resultant, the wave, $g_b(t)$, of Fig. XII-8b is obtained. The average value of this wave is independent of the period, T, and is equal to $v^2/2E$. Thus the output of the system as shown in Fig. XII-9 is proportional to $v^2(t)$. The bandwidth of this system is inversely proportional to the period, T, of the triangular wave, $g_a(t)$. By this technique, a large class of functions can be generated by properly shaping the pulses of the periodic wave. Thus if the variation of the width of a pulse is

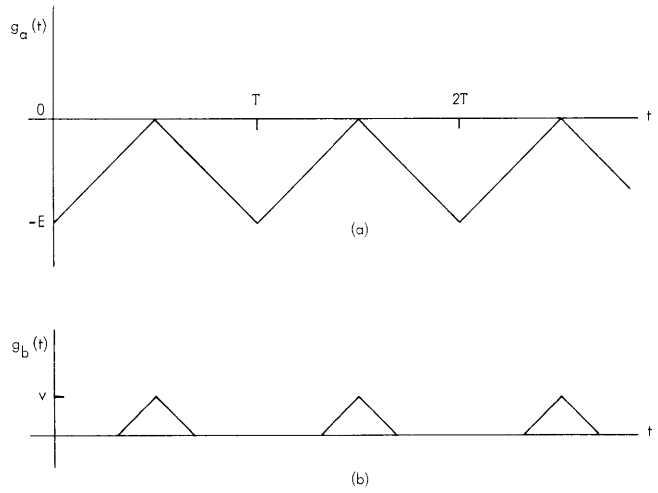

Fig. XII-8. (a) A negative triangular wave. (b) The wave $g_b(t)$ whose average value is $v^2/2E$.

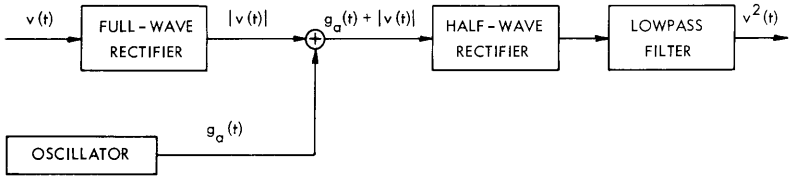

Fig. XII-9. Square-law device.

g(x), in which x is the distance from the peak of the pulse, then the average value of the wave depicted in Fig. XII-10 after half-wave rectification is equal to $\frac{1}{T}\int_0^v g(x)\,dx$. Now let $g(x) = f'(x)$. Then the average value of the rectified periodic wave can be expressed as $\frac{1}{T}f(v)$. For example, for a square-law device we require that $f(x) = x^2$, and thus we require $g(x) = f'(x)$ to be proportional to x. For an n^{th}-law device, we require that $f(x) = x^n$, and thus, for such a device, g(x) must be proportional to x^{n-1}. The output of a diode network for a triangular-wave input is one source of such a periodic wave of pulses.

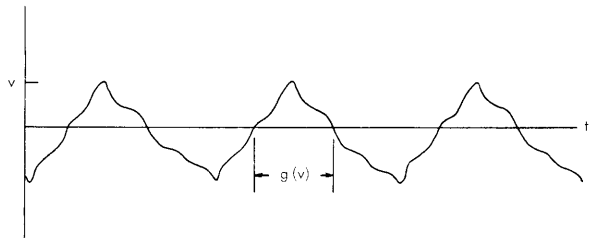

Fig. XII-10. Periodic wave pertinent to general function generation.

By the addition of simple circuits, many identical function generators can be constructed from one periodic-wave oscillator. For example, an additional square-law device can be obtained from the system of Fig. XII-9 simply with two additional rectifiers and a lowpass filter. Figure XII-11 is a schematic diagram of such a system. The two square-law devices of Fig. XII-11 are essentially identical, since they utilize the same periodic wave, $g_a(t)$, as the basis for their square-law character. This result,

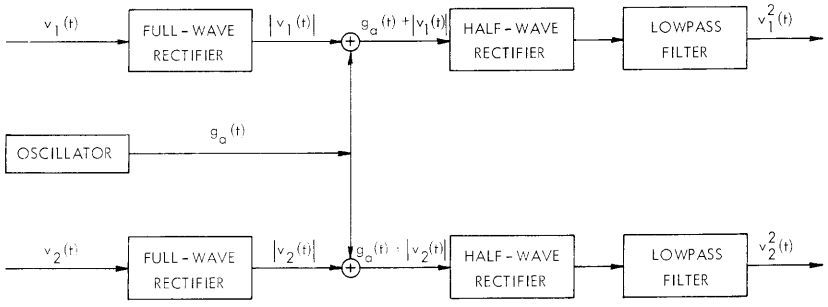

Fig. XII-11. Two square-law devices using the same periodic-wave oscillator.

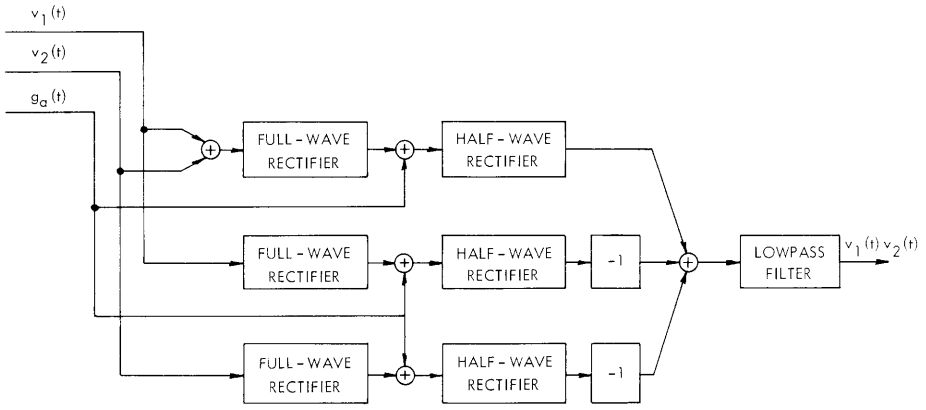

Fig. XII-12. A multiplier.

that the function generators are essentially identical, can be used to increase the accuracy of the function generator, since undesired nonlinearities can be eliminated. For example, a usual method of constructing a multiplier from square-law devices is to make use of the relation $4v_1v_2 = (v_1+v_2)^2 - (v_1-v_2)^2$. However, an error is introduced if the square-law device contains a linear kernel. Such an error can be eliminated by the system of Fig. XII-12, in which we have made use of the relation $2v_1v_2 = (v_1+v_2)^2 - v_1^2 - v_2^2$. The multiplier of Fig. XII-12 requires one more square-law device. However, the additional square-law device is obtained with just the addition of two rectifiers. In a similar manner, the output that is due to other undesired kernels can be eliminated (see Section XII-B).

M. Schetzen

D. OPTIMUM LAGUERRE FINITE-TERM EXPANSION OF FUNCTIONS

This report summarizes results obtained by Claude J. R. Deal and presented as a thesis to the Department of Electrical Engineering, M.I.T., September 1962, in partial fulfillment of the requirements for the degree of Master of Science.

Under certain general conditions, a function f(t) can be expressed as

$$f(t) = \sum_{n=1}^{\infty} a_n \phi_n(t), \tag{1}$$

in which $\{\phi_n(t)\}$ is a complete set of orthonormal functions so that

$$\int_{-\infty}^{\infty} \phi_n(t)\, \phi_m(t)\, dt = \begin{cases} 1 & m = n \\ 0 & m \neq n. \end{cases} \tag{2}$$

In physical applications, an upper limit of the number of terms that can be used in the series representation is determined by practical considerations. The truncated expansion thus differs from the actual function being expanded by an error, $\mathscr{E}_N(t)$, which is a function of N, the number of terms used in the expansion. This error is

$$\mathscr{E}_N(t) = f(t) - f_N(t), \tag{3}$$

in which

$$f_N(t) = \sum_{n=1}^{N} a_n \phi_n(t). \tag{4}$$

A measure of the size of this error is the integral-square error, E_N,

$$E_N = \int_{-\infty}^{\infty} \mathscr{E}_N^2(t)\, dt. \tag{5}$$

The values of the coefficients, a_n, for which the integral-square error is a minimum are given by

$$a_n = \int_{-\infty}^{\infty} f(t)\, \phi_n(t)\, dt. \tag{6}$$

An expression for the minimum integral-square error obtained by substituting the values of the coefficients as given by Eq. 6 in Eq. 5 is

$$E_N = \int_{-\infty}^{\infty} f^2(t)\, dt - \sum_{n=1}^{N} a_n^2. \tag{7}$$

The minimum integral-square error can always be made as small as desired by making N, the number of terms used in the expansion, sufficiently large. If, however, we set an upper limit to N, the integral-square error, E_N, given by Eq. 7 can be minimized by stretching or compressing the time scale of the orthonormal set. Analytically, the time scale of the orthonormal set can be stretched or compressed by replacing the variable t by pt, in which p is a positive constant. The new set, $\left\{\frac{1}{\sqrt{p}}\phi_n(pt)\right\}$, then also is orthonormal.

1. Optimum Laguerre Expansion

The problem of determining the optimum value of the scale factor, p, has been studied for the particular orthonormal set that is composed of the Laguerre functions.[1] A result of this study is a practical method by which we can locate all those values of the scale factor, p, for which the integral-square error, as given by Eq. 7, has a local minimum.

The set of Laguerre functions is orthonormal over the interval $(0, \infty)$. Also, each

Laguerre function is realizable as the impulse response of a linear system. This set, as well as others, with its network realizations has been discussed in detail by Lee.[2] The Laguerre set is obtained by forming an orthonormal set from the sequence of functions, $g_n(t)$,

$$g_n(t) = \begin{cases} (pt)^n e^{-pt} & t \geq 0 \\ 0 & t < 0 \end{cases} \qquad n = 0, 1, 2, 3, \ldots, \tag{8}$$

in which p is the scale factor. The first few terms and the general term of the Laguerre functions are

$$\begin{aligned} \ell_0(p,t) &= \sqrt{2p}\, e^{-pt} \\ \ell_1(p,t) &= \sqrt{2p}\,(2pt-1)\, e^{-pt} \\ &\vdots \\ \ell_n(p,t) &= \sqrt{2p}\left[\frac{(2pt)^n}{n!} - \frac{n(2pt)^{n-1}}{1!(n-1)!} + \frac{n(n-1)(2pt)^{n-2}}{2!(n-2)!} - \ldots + (-1)^n\right] e^{-pt}. \end{aligned} \tag{9}$$

The problem of interest is that of minimizing $E_N(p)$ which, from Eqs. 6 and 7, is

$$E_N(p) = \int_{-\infty}^{\infty} f^2(t)\, dt - \sum_{k=0}^{N-1} C_k^2(p) \tag{10}$$

and

$$C_k(p) = \int_0^{\infty} f(t)\, \ell_k(p,t)\, dt. \tag{11}$$

The values of p for which $E_N(p)$ is stationary can be obtained by differentiating Eq. 10 with respect to p and making use of the identity

$$\frac{\partial \ell_k(p,t)}{\partial p} = \frac{k}{2p}\, \ell_{k-1}(p,t) - \frac{k+1}{2p}\, \ell_{k+1}(p,t). \tag{12}$$

Then it is found after some algebra that $E_N(p)$ is stationary for those values of p for which

$$C_N(p)\, C_{N-1}(p) = 0. \tag{13}$$

Thus the stationary points of $E_N(p)$ can be determined experimentally by measuring the N^{th} coefficient of the Laguerre expansion, $C_{N-1}(p)$, and the $(N+1)^{st}$ coefficient of the Laguerre expansion, $C_N(p)$. The stationary points of $E_N(p)$ are those values of p for which either coefficient is zero. Information as to the nature of the stationary points can be obtained by observing the sign of the coefficients. Thus if the sign of the product, $C_N(p)\, C_{N-1}(p)$, changes at a root of Eq. 13, then the stationary point is either

a maximum or a minimum; if, on the other hand, the sign does not change at a root, then the stationary point is an inflection point.

Although the procedure derived does not yield the optimum value of p for which $E_N(p)$ is an absolute minimum, we do obtain a set of values of which one is the desired optimum value. The optimum value of p can be determined by measuring the integral-square error at all the critical values of p and choosing that value for which the integral-square error is a minimum. Since the number of critical values of p is usually small, this method is a definite improvement over having no criterion with which to select a value of p from its semi-infinite range. We might expect that if a function is to be expanded in a series containing only N terms, then, generally speaking, the minimum of the integral-square error should occur for a value of p at which the coefficient of the $(N+1)^{th}$ term is zero. However, examples have been obtained for which this is not true.[1] Therefore, in locating the value of p for which the integral-square error is an absolute minimum, one should measure the integral-square error at all values of p, as determined from Eq. 13, for which $E_N(p)$ has a relative minimum.

It should be noted that this technique of determining the optimum scale factor, p, requires knowledge only of the product $C_N(p)\,C_{N-1}(p)$ and does not require specific knowledge of the function being expanded. Thus, for example, this technique can be used to determine the optimum scale factor in the measurement of correlation functions by Laguerre series expansion.[3] Some experimental work was performed and the results were in agreement with those predicted.[1]

M. Schetzen

References

1. C. J. R., Deal, Optimum Laguerre Series Expansion of Functions, S.M. Thesis, Department of Electrical Engineering, M.I.T., September 1962.

2. Y. W. Lee, Statistical Theory of Communication (John Wiley and Sons, Inc., New York, 1960).

3. M. Schetzen, Measurement of correlation functions, Quarterly Progress Report No. 57, Research Laboratory of Electronics, M.I.T., April 15, 1960, pp. 93-98.

E. DESIGN AND ANALYSIS OF A DC TAPE RECORDING SYSTEM USING TWO-STATE MODULATION

1. Introduction

Since recording down to zero frequency cannot be achieved by direct means on conventional tape recorders, a low-frequency signal must be converted to a high-frequency form before it can be reproduced. An investigation of the application of two-state

modulation to the recording of dc signals is almost completed[1] and will be described in this report.

For the purpose of this investigation we consider two-state modulation to be the conversion of a slowly varying signal to a rectangular wave that is symmetric about zero and has a duty cycle of average value very nearly proportional to the instantaneous value of the input. The frequency of this wave is much higher than the highest frequencies present in the input and may be dependent upon the instantaneous value of the input signal. Demodulation is achieved by passing the two-state signal through a lowpass filter that removes the higher frequency components of the wave and leaves the desired output.

A specific modulation system, being developed by Bose,[2] was used for much of the investigation. Since the noise introduced by this modulation process is much less than that introduced by the recording process, we assumed a noiseless modulation system. Our objectives were to design and build a detecting system for restoring the two-state wave from the recorder output so that noise in the demodulated output resulting from the recorder noise would be minimized, and to determine limitations on the over-all system performance imposed by this recorder noise.

2. Basic Operation of the System

A block diagram of the system is shown in Fig. XII-13. The two-state signal f(t) from the modulator is recorded. The recorder output r(t) consists of an alternating positive-negative train of approximately Gaussian-shaped pulses as shown in Fig. XII-14.

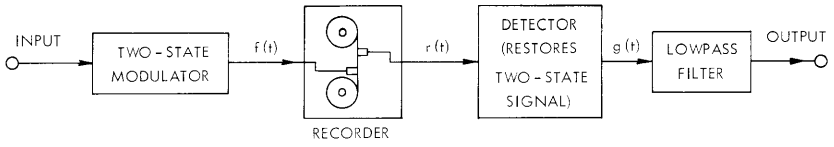

Fig. XII-13. The dc recording system.

The significant noise introduced by the recorder is not additive but appears in two forms: (a) a multiplicative random amplitude modulation of the pulse train, and (b) a random sideways displacement of the individual pulses of the output train. This noise is chiefly due to mechanical fluctuations in the tape drive mechanism. It was observed that appreciable amplitude variations occur over time intervals that are much longer than the pulse width.

Regardless of the detecting system used for restoring the two-state wave from the recorder output, a certain amount of jitter in the zero crossings of the restored wave

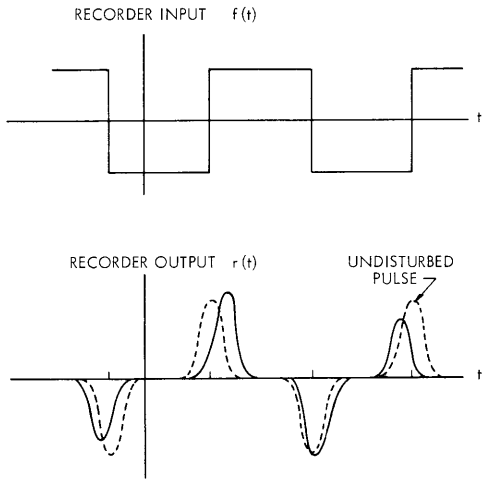

Fig. XII-14. Recorder input and output showing typical recorder noise.

g(t) will appear because of the variation in the pulses of r(t). Therefore we desire a detecting system that restores the two-state signal so that jitter introduced into the zero crossings of g(t) is minimized.

3. Detector Construction

The detector for restoring the two-state signal from the recorder output was constructed by using a standard sequence of Digital Equipment Corporation modules. This system would locate a pulse of r(t) by detecting the position of the zero slope point at the peak of that pulse. A bistable multivibrator would be triggered on or off, the state depending on the polarity of that pulse. Thus the two-state wave is restored. Details of construction are presented in the author's thesis.[3]

A feature of pulse location by peak detection is that the determined position is practically independent of the random amplitude-modulation noise from the recorder.

4. Analysis of the Output Noise

A theoretical analysis was performed to relate the noise appearing in the demodulated output to the zero-crossing jitter of g(t) introduced by the recorder noise.[1] We consider g(t) to be a square wave (this is the case for zero input) which has its zero-crossings phase modulated by a continuous random signal x(t). Specifically, a zero crossing ordinarily occurring at $t = \frac{kT}{2}$ in the absence of jitter occurs at $t = \frac{kT}{2} + x\left(\frac{kT}{2}\right)$, as shown in Fig. XII-15. The following restrictions are placed on x(t):

(a) x(t) must be wide-sense stationary, and

(b) $\max |x(t)|$ must be less than $\frac{T}{4}$ to ensure that the i^{th} zero crossing occurs before the j^{th} when $i < j$.

Under these conditions the power density spectrum of g(t) for $|f| < \frac{1}{T}$ was computed and is given by

$$S_n(f) \simeq \frac{16A^2}{T^2} \sum_{k=-\infty}^{\infty} S_x\left(f - \frac{2k+1}{T}\right) \tag{1}$$

or alternatively by

$$S_n(f) \simeq \frac{8A^2}{T}\left[R_x(0) + 2\sum_{k=1}^{\infty} (-1)^k R_x\left(\frac{kT}{2}\right) \cos k\pi Tf\right], \tag{2}$$

where $|f| \ll 1/\max|x(t)|$. Here, $S_x(f)$ is the power density spectrum of x(t), $R_x(\tau)$ is the autocorrelation of x(t), T is the period of the unjittered square wave, and A is the amplitude of g(t).

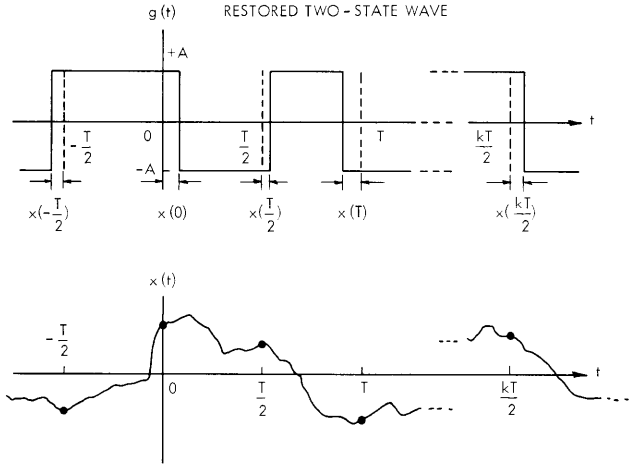

Fig. XII-15. Jittered square wave illustrating the process x(t).

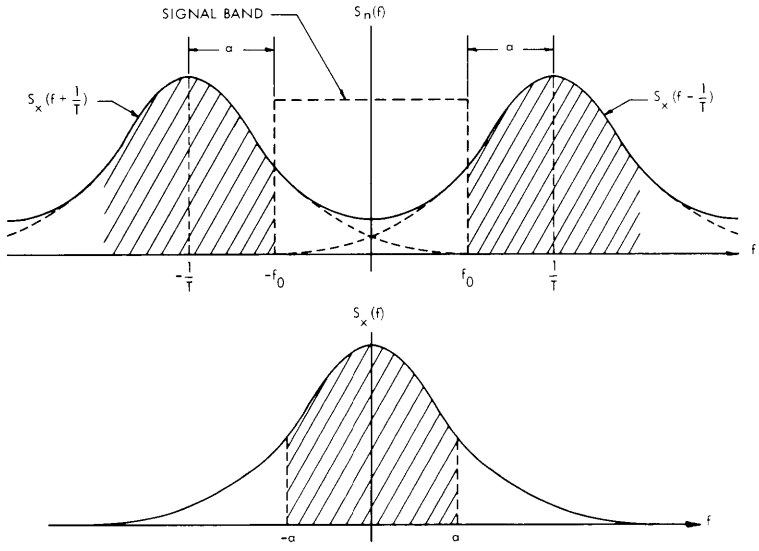

Fig. XII-16.

Output noise spectrum. (Power within the shaded area lies outside the signal band, $|f| < f_o$.)

The two representations of $S_n(f)$ are equivalent; the second is the Fourier series for the first. When power in x(t) is concentrated in low frequencies so that the shifted spectra of $S_x(f)$ do not overlap appreciably, the first form is more convenient than the second; when the jitter on different zero crossings is relatively uncorrelated, most of the Fourier coefficients become negligible and the Fourier series is the more convenient expression. An example of $S_n(f)$ is shown in Fig. XII-16.

5. Application of the Analysis to the Recording System

Referring to Fig. XII-16, we see that power in x(t) at frequencies below $\alpha = \frac{1}{T} - f_o$ does not produce amplitude noise in our signal band $|f| \leq f_o$, where $0 < f_o < \frac{1}{T}$. That is, power in the shaded portions of the spectra shown in Fig. XII-16 lies outside the signal band. This result implies that "wow" and "flutter" (terms commonly used to describe effective tape speed variations resulting from both recording and reproducing) at frequencies below α will not contribute amplitude noise to the demodulated output.

In a typical recording application, $\frac{1}{T}$ = 3000 cps, f_o = 300 cps, and α = 2700 cps. Therefore, wow and flutter below 2700 cps would not produce amplitude noise in the final output. There will, however, be time-base variations in the output, but for many applications this effect can be tolerated.

This result indicates that significant improvement in noise characteristics is to be obtained when a tape drive system designed particularly for the elimination of high-frequency flutter is used.

The spectrum of the output noise of the system constructed for this investigation was measured. The theoretical results given above were used to interpret these measurements.

For zero input and a 1-volt amplitude, 3-kc modulation carrier, a 290-μv rms noise voltage over a 0-300 cps bandwidth was measured. For a 0.75-volt dc signal the corresponding signal-to-noise ratio would be approximately 68 db.

D. E. Nelsen

References

1. D. E. Nelsen, Design and Analysis of a D-C Tape Recording System Using Two-State Modulation, S. M. Thesis, Department of Electrical Engineering, M. I. T., August 1963.

2. A. G. Bose, A two-state modulation system, Quarterly Progress Report No. 66, Research Laboratory of Electronics, M. I. T., July 15, 1962, pp. 187-189; Quarterly Progress Report No. 67, pp. 115-119; Quarterly Progress Report No. 70, pp. 198-205; paper presented at the 1963 Western Electronic Show and Convention, San Francisco, California, August 20-23, 1963.

3. D. E. Nelsen, op. cit., Appendix I.

F. EXPERIMENTAL INVESTIGATION OF THRESHOLD BEHAVIOR IN PHASE-LOCKED LOOPS

The phase-locked loop is a nonlinear feedback system that can be represented by the following mathematical model. (See Fig. XII-17.) The phase-locked loop has been mathematically analyzed in published data. These models include both linearized models and various models that take into account the essentially nonlinear nature of the phase-locked loop.[1, 2]

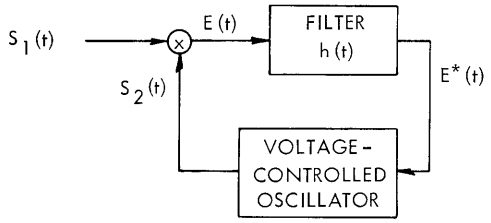

SYSTEM SIGNALS

$$S_1(t) = \sqrt{2}\, A \sin(wt + \theta_2) + N(t)$$

$$S_2(t) = \sqrt{2} \cos(wt + \theta_2)$$

$$E(t) = S_1(t)\, S_2(t)$$

$$E(t) = A \sin(\theta_1 - \theta_2) + \sqrt{2}\, N(t) \cos(wt + \theta_2) + f(2w)$$

$$E^*(t) = \int_{-\infty}^{\infty} h(\tau)\, E(t-\tau)\, d\tau$$

$$\frac{d\theta_2}{dt} = K_v E^*(t)$$

Fig. XII-17. Phase-locked loop.

We have experimentally measured the variance of the phase difference $\theta = (\theta_1 - \theta_2)$ of a laboratory model phase-locked loop to compare this measured variance with the variances of θ calculated by the various theoretical analyses.[3]

The variance of θ is plotted against the coherent noise-to-signal ratio in the noise passband of the loop. This coherent noise-to-signal ratio is $N_o K/4A^2$. Here, $N_o/2$ is the height of the double-sided power density spectrum of the additive noise of the input that is N(t) in Fig. XII-17. K is the open-loop gain of the phase-locked loop. A is the rms voltage of the input sinusoid.

The noise-to-signal ratio is then $\frac{1}{2}\left(\frac{N_o K}{2A^2}\right)$.

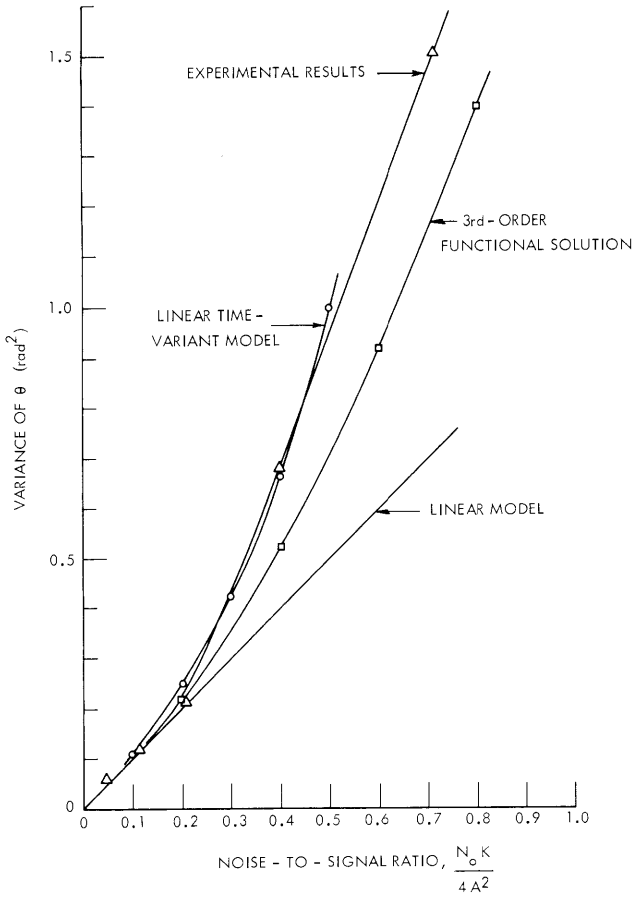

Fig. XII-18. Theoretical and experimental results.

The curves plotted in Fig. XII-18 are the results of theoretical analyses for the linear model, the linear randomly time-variant model,[1] the third-order functional model,[2] and the experimental results.[3] All of these curves are for first-order loops. It is noted that the experimental results agree closely with the linear model below threshold and with the linear randomly time-variant model for the threshold region and above.

The experimental and theoretical results have been discussed in detail.[1-3]

A. G. Gann

References

1. H. L. Van Trees, A lower bound on stability in phase-locked loops, Information and Control 6, 195-212 (1963).

2. H. L. Van Trees, Functional Techniques for the Analysis of the Nonlinear Behavior of Phase-Locked Loops, paper presented at the 1963 Western Electronic Show and Convention, San Francisco, California, August 20-23, 1963.

3. A. G. Gann, Experimental Investigation of Threshold Behavior in Phase-Locked Loops, S.M. Thesis, Department of Electrical Engineering, M.I.T., June 1963.

G. MULTIPLEX COMMUNICATION SYSTEM USING PSEUDO-NOISE CARRIERS

This report summarizes the results of a study that has been submitted to the Department of Electrical Engineering, M.I.T., as a joint thesis in partial fulfillment of the requirements for the degree of Master of Science for J. K. Omura and for the simultaneous degrees of Master of Science and Electrical Engineer for A. J. Kramer.

1. Introduction

The aim of this research was to build an experimental two pseudo-noise carrier system for studying some of the properties of its behavior.

The advantages of the wideband pseudo-noise communication system are well known. A major disadvantage of the pseudo-noise carrier scheme is that it is relatively wasteful of channel bandwidth. In order to compensate for the large bandwidth, several wideband carriers may be put in the same frequency band. If a conventional demodulation technique is used, each carrier acts as an uncorrelated noise to every other carrier. Van Trees[1] has derived an efficient demodulation technique for an analog pseudo-noise system. The experimental system reported here was based on this efficient demodulation technique.

The results of this work indicate that the idea of the efficient demodulation technique is basically sound and that an extension to more than two pseudo-noise carriers is warranted.

Several important design considerations for efficient system operation have been determined.

Figure XII-19 is a block diagram of the efficient one-message pseudo-noise carrier

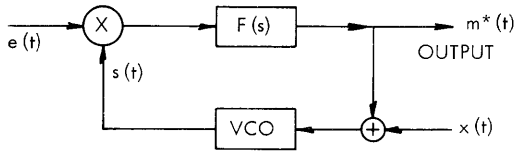

$$e(t) = A \sin\left[w_o t + \int_{-\infty}^{t} x(u)\,du + \int_{-\infty}^{t} m(u)\,du\right] \quad \text{Pseudo-Noise Carrier}$$

$$s(t) = \cos\left[w_o t + \int_{-\infty}^{t} x(u)\,du + \int_{-\infty}^{t} m^*(u)\,du\right]$$

$x(t)$ = Pseudorandom Signal
$m(t)$ = Modulation Signal
$m^*(t)$ = Output
VCO = Voltage-Controlled Oscillator
$F(s)$ = Realizable Filter Transfer Function

Fig. XII-19. Single-message pseudo-noise demodulator.

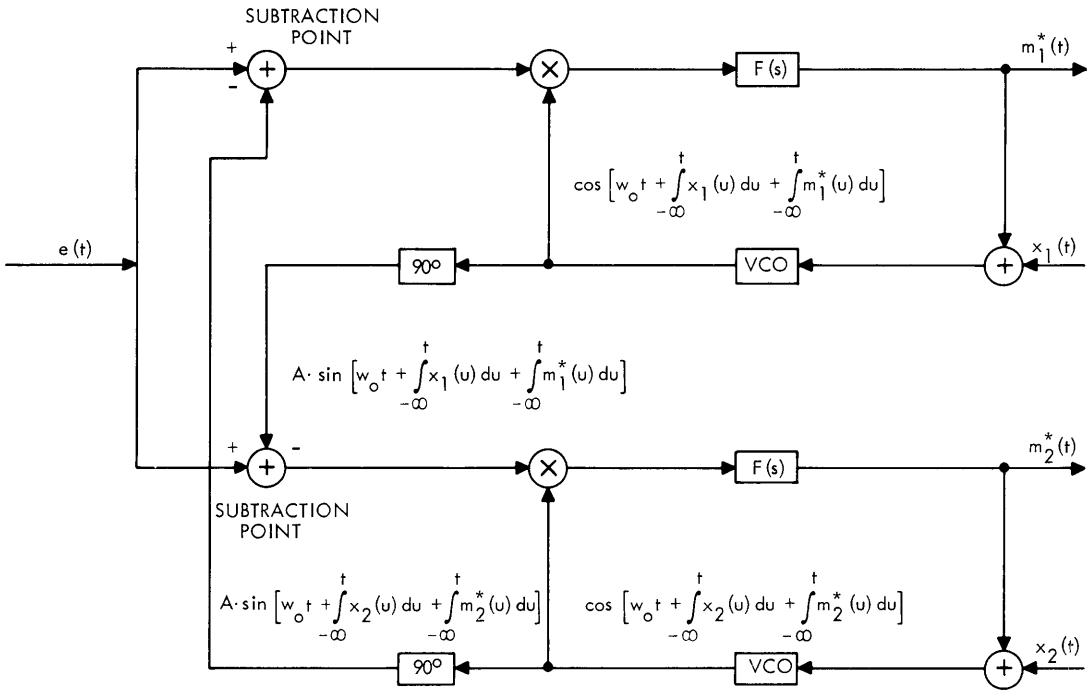

Fig. XII-20. Two-message pseudo-noise demodulator.

demodulator, and Fig. XII-20 is a block diagram of the efficient two-message pseudo-noise carrier demodulator.

Only a brief explanation of the results will be given in this report. More details on the operation of the two pseudo-noise carrier system and the experimental results may be found in the authors' thesis.[2]

2. Discussion of Results

All data presented here were taken with no modulation. The transmitted pseudo-noise carriers are 20 kc wide with center frequency at 70 kc.

Figure XII-21 shows the performance of a single standard phase-lock loop discriminator with a sine-wave carrier used. This performance serves as a standard of comparison of the performance of the two-message pseudo-noise system.

In Fig. XII-22 we have the performance of a single-message pseudo-noise carrier demodulator. This system has a wideband carrier. Two such wideband pseudo-noise signals are demodulated by the efficient two-message demodulator of Fig. XII-20. Note that this demodulator contains two single-message pseudo-noise demodulators with interconnecting subtraction points. Figure XII-23 shows its performance. By comparing its performance with the standard system and with the single-message pseudo-noise system, we can determine how well the multiplex system works when we have the

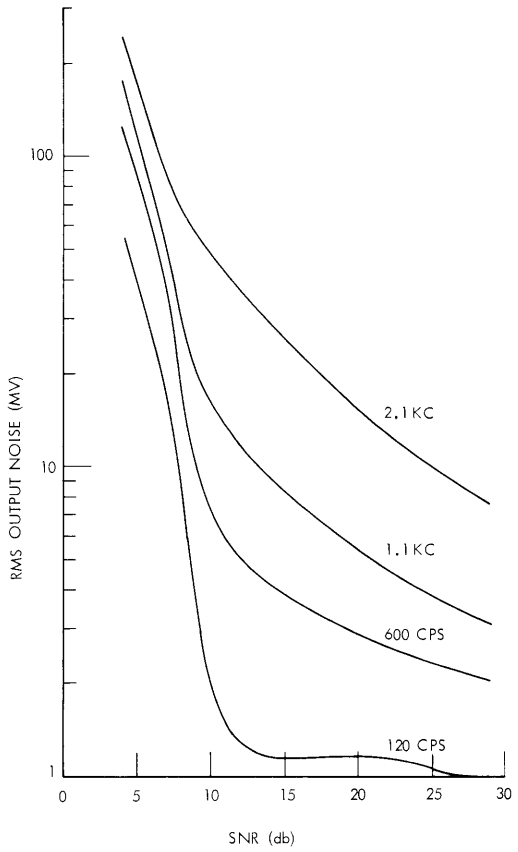

Fig. XII-21. Performance of a standard system.

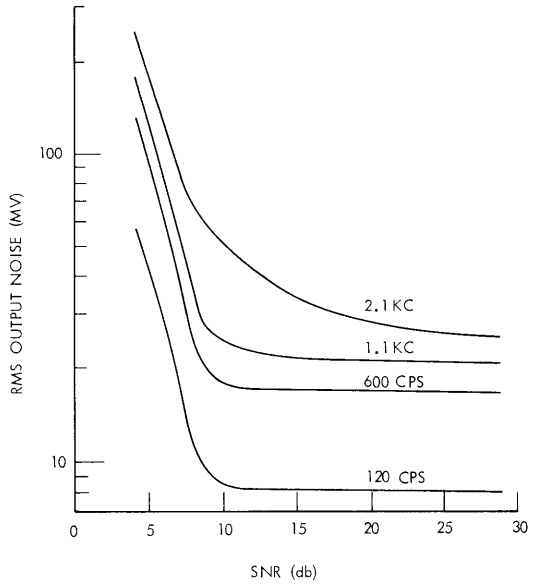

Fig. XII-22. Performance of a single-message pseudo-noise system.

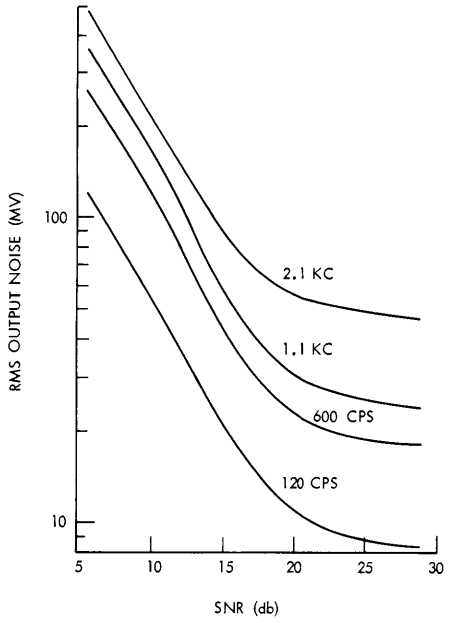

Fig. XII-23. Performance of a two-message pseudo-noise system.

simultaneous transmittal of two pseudo-noise carriers.

The ordinate of Figs. XII-21-XII-23 is the rms noise output in millivolts. The abscissa is the power signal-to-noise ratio (SNR) at the input of the discriminator. Additive white Gaussian noise was used. The parameter of the various curves is the cutoff frequency of the lowpass filter at the outputs.

In all of the figures we can see a point at which the noise output of the demodulator starts to increase rapidly. This increase is due to loss of lock with the incoming signal when the noise at the input becomes too large.

In comparing Fig. XII-21 with Fig. XII-22, we see how much noise is generated by slight inaccuracies of the demodulator in matching the pseudo-noise carrier at the demodulator to the incoming pseudo-noise carrier. Figure XII-23 shows the noise that is due to both incorrect pseudo-noise matching and interference of the two input signals with each other. The interconnecting subtraction points eliminate most of the interfering pseudo-noise signal to each single-message demodulator.

We observe that, when the signal-to-noise ratio is high, the two-message system works almost as well as the one-message system. As one would expect, the threshold in the two-message system is higher.

3. Conclusion

Enough information was obtained to show that the basic idea for an efficient demodulator of a multiplex pseudo-noise system is feasible. The experimental data show that good subtraction of the interfering pseudo-noise signal is very important. In

the laboratory system the most important area of improvement is better front-end subtraction.

The experimental results indicate that an extension of the two pseudo-noise carrier system is warranted. This will not present any important problems that have not already been encountered in the two-carrier system. A block diagram of an n-message pseudo-noise system has been given.[3]

A. J. Kramer, J. K. Omura

References

1. H. L. Van Trees, An Efficient Demodulator for an Analog Pseudo-Noise Multiplex System, Report 65G-3, Lincoln Laboratory, M.I.T., July 2, 1963.

2. A. J. Kramer and J. K. Omura, A Multiplex Communication System Using Pseudo-Noise Carriers, S.M. Thesis, Department of Electrical Engineering, M.I.T., August 19, 1963.

3. H. L. Van Trees, op. cit.; see Fig. 1.